

# Development and Application of a Parametric Design Tool for Design Iterations of Large Turboprop Aircraft

Martin E. Kügler\* and Niclas P. Randt†

Technical University of Munich, 85748 Garching, Germany

In the context of an increasing congestion of air traffic flows worldwide, a high-capacity turboprop transport aircraft was designed at the Institute of Aircraft Design of Technical University of Munich that is specifically aimed at serving short- and mid-range routes. Within the scope of research on the concept, this paper presents a parametric aircraft design tool that was created at the institute to support comprehensive analyses and design iterations of large turboprop aircraft. Through a modular approach, the tool covers a broad range of design-related disciplines including aerodynamics, mass prediction, and propulsion and performance modeling. The tool was employed to examine the institute’s turboprop concept. It revealed critical design features and drivers of the concept. During multiple design loops, parameter variations were carried out, and the aircraft was redesigned until the top-level aircraft requirements and certification constraints were met. Finally, mission performance and fuel efficiency of the revised concept were evaluated with the tool.

## Nomenclature

$AR$	= aspect ratio	$S_{ref}$	= wing reference area
$C_{D0}$	= zero-lift drag coefficient	$S_{wet}$	= wetted area
$C_{Di}$	= drag-due-to-lift coefficient	$T$	= thrust
$C_f$	= flat-plate skin-friction coefficient	$T_S$	= static thrust
$C_L$	= lift coefficient	$V$	= velocity
$C_{La}$	= lift-curve slope	$W_{TO}$	= take-off weight
$F$	= fuselage lift factor	$\alpha$	= angle of attack
$FF$	= component form factor	$\beta$	= Prandtl-Glauert factor
$K$	= drag-due-to-lift factor	$\eta_{airfoil}$	= airfoil efficiency
$P_{eq}$	= equivalent engine power	$\eta_{effective}$	= effective propeller efficiency
$Q$	= interference factor	$\Lambda_{max\ thickness}$	= wing sweep angle at max. airfoil thickness
$S_{exposed}$	= exposed wing planform area		

## I. Introduction

THE continuously growing demand for worldwide air transport and globally observable urbanization trends are leading to an increasing congestion of air traffic flows, especially between major hub airports. In the three major air transport regions of the world (i.e., North America, Asia/Pacific, and Europe), further growth of the aviation sector is increasingly limited by aircraft-handling capacities both on the ground and in the air. This has resulted in a trend towards employing larger aircraft with an increased passenger capacity on short routes.<sup>1</sup>

### A. High-Capacity Aircraft for Short- to Medium-Range Operation

Currently operating large aircraft are generally designed for long-haul operation. However, the vast majority of commercial flight operations cover short- to medium-haul routes. Here, Kenway et al. demonstrated that large aircraft being specifically designed for short- to mid-range operations are capable of providing economic and ecological benefits compared to both current narrow-body and wide-body types of aircraft, independent of the technological innovation level.<sup>2</sup>

\*Research Assistant, Institute of Flight System Dynamics, Boltzmannstrasse 15, AIAA Student Member.

†Research Assistant, Institute of Aircraft Design, Boltzmannstrasse 15, AIAA Student Member.

At the Institute of Aircraft Design of the Technical University of Munich, the potential of operating such specifically designed high-capacity aircraft on short- to medium-range routes is investigated using a scenario-based global fleet system dynamics model.<sup>3</sup>

In this context, on the basis of a profound market analysis, the preliminary design of a high-capacity turboprop-powered transport aircraft has been developed as a demonstrator and application case for the analyses. The concept is aimed at carrying a payload of 420 passengers and five tons of cargo over a distance of 1,620 NM (3,000 km) enabling the aircraft to serve more than 90% of the current short- and medium-range routes.<sup>4</sup> The configuration was named ‘Propcraft P-420’



**Figure 1. Visualization of the investigated high-capacity turboprop aircraft concept Propcraft P-420.<sup>4</sup>**

and is shown in Fig. 1. It features a conventional low-wing layout with four wing-mounted engines and a twin-deck passenger cabin. The aircraft was conceptualized with turboprop engines in order to maximize its fuel efficiency. In combination with a slightly reduced cruising speed, this type of engine promises higher fuel efficiency than can be attained with turbofan engines.<sup>5</sup> The four engines of the concept were projected with an equivalent power rating of 9,700 kW each and dual-stage counter-rotating propellers. Besides ecological and economic advantages, the concept emphasizes operational flexibility. Because a high application potential for the concept was seen in the emerging markets of the Asia/Pacific region, aircraft dimensions, take-off and landing performance, as well as boarding and deboarding facilities were designed to enable operation on airfields with limited infrastructure. In order to allow for a comparison of performance and fuel efficiency of the concept to the current airline fleet, the entire design was based on currently available technologies only.

## B. Parametric Design Phase

The above-described baseline version of the high-capacity aircraft concept was the outcome of the conceptual phase of the aircraft design process as outlined by Torenbeek<sup>6</sup> and shown in Fig. 2.

This paper presents the subsequent analyses and parametric redesign of the baseline aircraft concept that were carried out within the scope of the preliminary design phase enframed in Fig. 2. Here, starting from the baseline design, a detailed analysis of the concept’s properties and performance was accomplished.

In the form of design iterations, the concept was developed further until a stage was reached where the design was considered sufficiently mature. The configuration development phase was then concluded with a technical description of the concept, which provides a basis for the future detailed design of the concept as well as its integration into the global fleet system dynamics model.

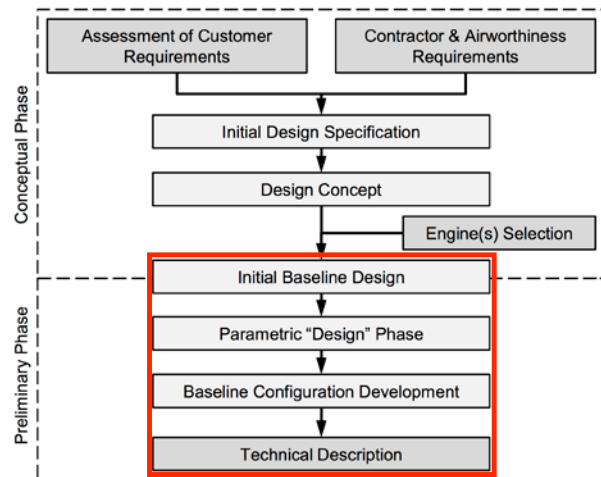


**Figure 2. Phases of the aircraft design process.<sup>6</sup> The scope of this paper covers the enframed preliminary phase.**

## C. Methodological Approach

With the goal to comprehensively assess and conduct design iterations of the P-420 concept, a parametric design tool was developed. The tool is tailored to handle large turboprop aircraft configurations. Based on a parametric definition of the aircraft configuration to be analyzed, the methodological framework of the tool features calculation techniques and models in distinct modules that determine aerodynamic properties, masses, and propulsion characteristics of the concept under scrutiny. The results obtained are then joint in a performance module that allows substantial statements on operational characteristics and fuel efficiency of the concept.

The comprised calculation methods of the tool are based on common conceptual and preliminary design practices,<sup>5,6,7</sup> and extended by further models and calibration data of the institute. Section II of this paper gives a detailed overview of the design tool and the methodology applied.

Eventually, the tool was successfully employed to evaluate the baseline concept of the P-420. With respect to the relevant design requirements and certification constraints, critical aspects and design drivers of the concept were identified. Section III of this paper shows and discusses the results obtained within this context. Finally, based on parametric design iterations that were carried out with the tool, a revised concept of the P-420 could be achieved.

## II. Integrated Design Tool for Large Turboprop Aircraft

The ‘Integrated Design Tool (IDT)’ was developed in a MATLAB environment. The tool is hence executable on any MATLAB-compatible system and provides a convenient accessibility of the source code as well as interfaces for data in-/output. The source code of the IDT is structured according to the different modules of the tool: Aircraft concept definition, aerodynamic analysis, mass estimation, propulsion modeling, and aircraft performance analysis. Fig. 3 shows a flow chart of the IDT with the input data required, calculation modules, and output results.

The input data are a set of parameters that provide a comprehensive definition of the aircraft concept to be investigated. At the current stage of development, the IDT is capable of modeling conventional transport aircraft configurations with low wings and turboprop engines in a subsonic flight regime. The input parameters cover the dimensions of the main components of the aircraft (wings, horizontal and vertical tail, fuselage, cabin, landing gear and engines). Furthermore, general configuration parameters are required such as passenger capacity, engine power, and the design mission profile.

In a first step, the IDT automatically calculates further relevant parameters from these input data covering geometric characteristics (e.g., aspect ratio, mean aerodynamic chord, and atmospheric properties) for the different phases of the design mission.

The main part of the IDT is labeled ‘Aircraft Concept Analysis’ in Fig. 3. The calculation methods of the contained analysis modules of the IDT are explained in the following and related references are given. The results of the analyses of the aircraft under investigation are provided by the IDT through both numerical values being displayed in the MATLAB command window and a set of plots and diagrams visualizing important characteristics (e.g., drag polars, engine characteristics, payload-range diagram).

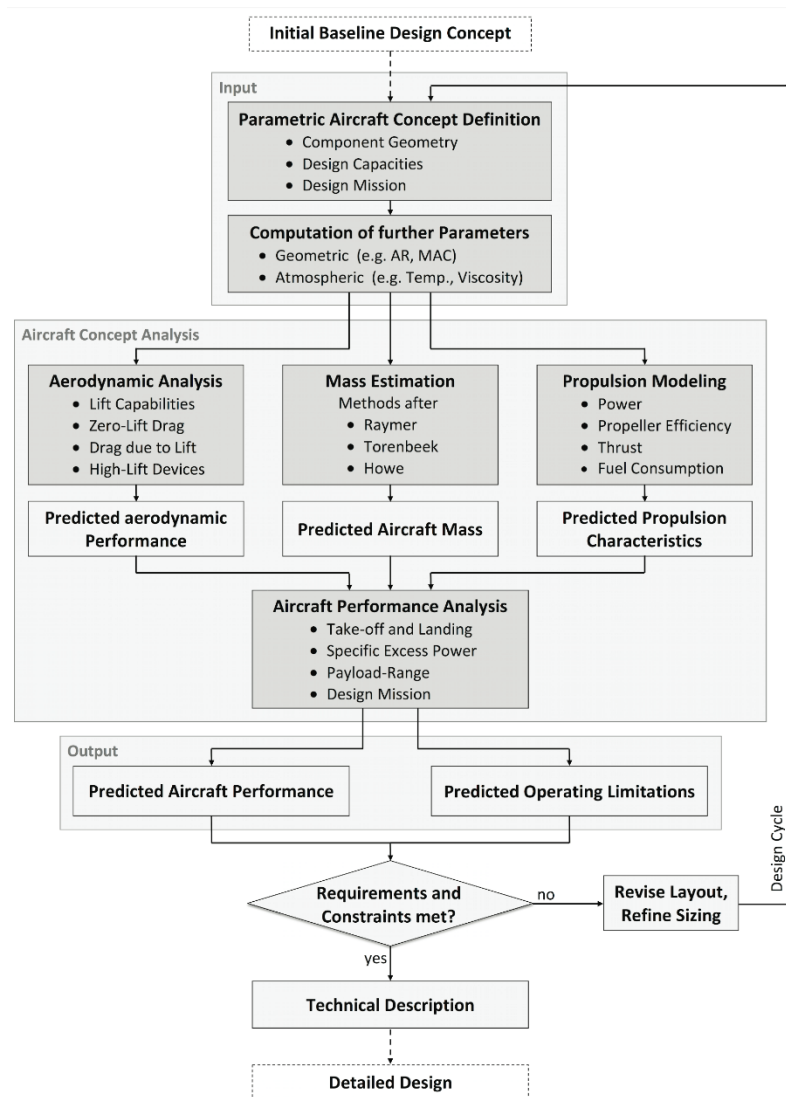


Figure 3. Flow chart of the IDT and the context of its application to the design process of the Propcraft P-420 concept.

## A. Aerodynamic Analysis

Key aspects covered by the aerodynamic analysis are the determination of lift, drag, and high-lift device characteristics in all relevant phases of flight. Several different calculation methods were implemented in the IDT in order to allow for comparisons and an assessment of the accuracy.

$$C_{L\alpha} = \frac{2\pi AR}{2 + \sqrt{4 + \frac{AR^2\beta^2}{\eta_{airfoil}^2} \left(1 + \frac{\tan^2 \Lambda_{max\ thickness}}{\beta^2}\right)}} \frac{S_{exposed}}{S_{ref}} F \quad (1)$$

The calculation starts with a two-dimensional airfoil and a three-dimensional wing analysis, and evaluates lift characteristics for specified slow-and-low and cruise flight conditions. The lift curve is calculated according to Lowry and Polhamus<sup>8</sup> (Eq. 1) with an estimation of the maximum achievable lift according to Finck et al.<sup>9</sup> The effect of high-lift devices is determined for leading-edge slats plus single- and double-slotted Fowler flaps using Raymer's approach.<sup>7</sup>

Drag analysis is subdivided into zero-lift drag, drag due to lift, and high-lift device drag increments. For zero-lift drag, an equivalent skin-friction method,<sup>7</sup> a semi-empirical estimation after Howe,<sup>5</sup> and a more comprehensive component buildup method<sup>7</sup> are implemented in the IDT. The basic equation of the component buildup method (Eq. 2) sums the drag of each aircraft component calculated from a flat-plate skin-friction coefficient, a form factor, and an interference factor. Increments are designated for miscellaneous special features  $C_{D,misc}$  (e.g., an upswept aft-fuselage) and leakages and protuberances  $C_{D,L\&P}$  of the aircraft.

Several drag calculation methods are implemented in the IDT to enable comparisons. For the investigation of the P-420 this component-buildup method was selected for zero-lift drag prediction.

$$C_{D0} = \frac{\sum C_{f,c} FF_c Q_c S_{wet,c}}{S_{ref}} + C_{D,misc} + C_{D,L\&P} \quad (2)$$

The lift-induced drag coefficient is estimated proportional to the square of the lift coefficient (Eq.3). For the calculation of the induced-drag factor K, the IDT features statistical methods after Howe<sup>5</sup> and Nita and Scholz,<sup>10</sup> an Oswald-span-efficiency method,<sup>7</sup> plus an advanced leading-edge-suction method<sup>7</sup> that takes viscous separation into account. This leading-edge-suction approach is employed for drag-due-to-lift calculations of the P-420 concept. Drag increments due to high-lift devices are calculated separately for zero-lift and lift-dependent drag as suggested by Raymer.<sup>7</sup> A composition of the results of the aerodynamic analysis of the baseline P-420 is depicted in Fig. 4, which shows the drag polar of the aircraft concept for different high-lift-device and landing-gear settings.

$$C_{Di} = KC_L^2 \quad (3)$$

## B. Mass Estimation

The mass-prediction module of the IDT determines the operating empty mass of the aircraft under investigation. It comprises several estimation methods with a varying level of detail and from different references. All of the methods were statistically derived by the respective author through regression analyses and are based on a component breakdown of the aircraft. A standardized format for this breakdown is provided by a 'Group Weight Statement' as depicted in Table 1. For each component, an individual estimation of the respective weight is calculated. Thereby, the selection of parameters that are taken into account varies with the method.

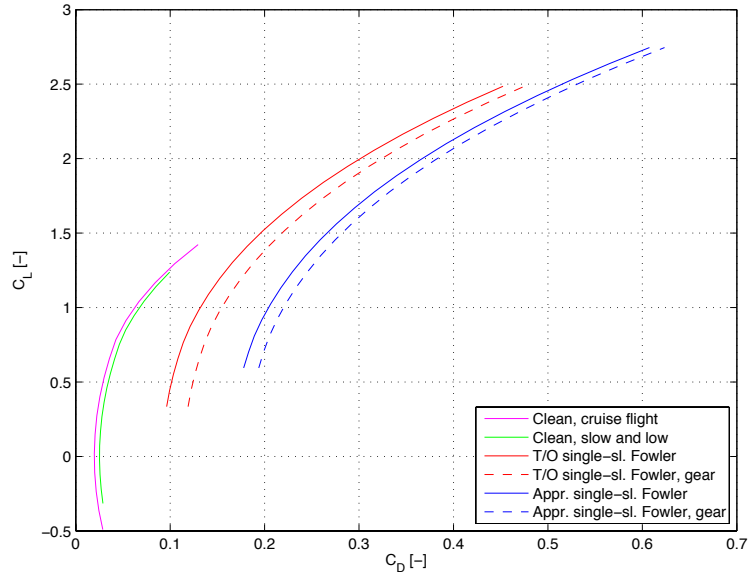


**Figure 4. Drag polars of the baseline Propcraft P-420 concept.** Colored lines represent different high-lift-device and landing-gear settings.

In total, the mass-estimation module of the IDT comprises six methods. Raymer's<sup>7</sup> approach features a comparably detailed breakdown and applies physics-based models in addition to the statistical equations. Two different predictions are provided by Torenbeek,<sup>6</sup> a simple one with a basic breakdown and a limited number of parameters plus a detailed method with an exhaustive breakdown and an extensive set of parameters. In his more recent work,<sup>11</sup> Torenbeek published another less detailed method, which is also implemented in the IDT. Besides, a basic and a more detailed mass estimation are provided by Howe.<sup>5</sup>

The component masses predicted are eventually summed up to group weights, which in turn yield the operating empty mass (cf. Table 1). For some structural items, reduction factors are introduced to allow for weight decimation due to the application of advanced composite materials.<sup>7</sup>

For the mass prediction of the baseline P-420, the detailed method after Torenbeek was selected. Due to its level of detail, it best represents the characteristics of the configuration, especially the double-deck cabin layout and the turboprop engines. The determined operating empty mass of 97.3 tons is about 7% greater than previously projected and yields a take-off mass of 172.2 tons.

**Table 1. Component mass breakdown of the baseline Propcraft P-420 concept. Detailed mass prediction after Torenbeek.<sup>6</sup>**

Component or group	Composites factor – where applicable –	Predicted mass in kg
<b>Structures:</b>		<b>44,148</b>
Wing	0.85	13,486
Fuselage	0.9	16,027
Horizontal and vertical tail	0.83	2,146
Landing gear	0.95	6,560
...		...
<b>Propulsion:</b>		<b>22,373</b>
Engines		7,600
Installation (incl. propellers)		12,288
...		...
<b>Systems and Equipment:</b>		<b>24,289</b>
Hydraulics and pneumatics		1,717
Electrical system		2,174
Furnishings		16,709
...		...
<b>Miscellaneous (e.g., paint)</b>		<b>963</b>
<b>Operational items (e.g., crew)</b>		<b>5,531</b>
<b>Operating mass empty</b>		<b>97,305</b>

### C. Propulsion Modeling

To account for aircraft propulsion, the IDT comprises a turboprop engine model. It captures the characteristics of the gas turbine and propeller throughout the aircraft operating range. Relevant parameters are the available shaft power of the turbine with its corresponding fuel consumption, the propulsive efficiency of the propeller that is strongly affected by the flight speed in relation to the propeller's rotational speed, and the attainable thrust that acts on the aircraft. Since corresponding data are not available for high-performance turboprop engines (i.e., engines with an equivalent take-off power around 10 MW, as required for the Propcraft P-420), own models had to be developed.

The characteristics of the available engine power were derived from published data of the Allison 501-M7 (T56-A-15) turboprop engine (rated at 3.7 MW of equivalent power).<sup>12</sup> Major influences are the ram effect that increases the turbine's overall pressure ratio and thus the supplied power with growing flight speed, and the decreasing air density at higher operating altitudes, which reduces engine power. Fig. 5 shows these characteristics, for which an analytic model was derived at the institute.<sup>4</sup>

A model for the engine fuel consumption was also developed based

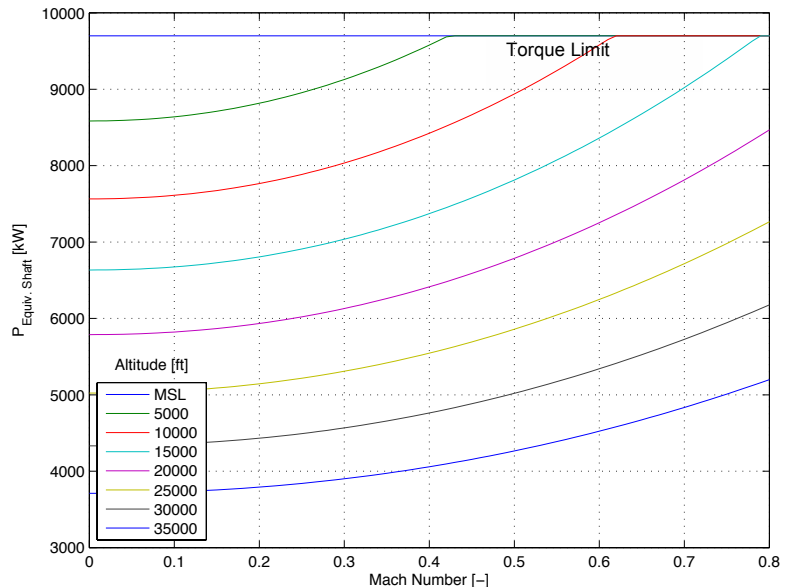


**Figure 5. Equivalent power characteristics of a single engine of the baseline Propcraft P-420 concept. Colored lines represent different flight**

on published data of the Allison engine. Again, an analytic model was derived through a regression analysis. Relevant characteristics are decreasing fuel consumptions with both rising flight speeds and higher altitudes.

The propulsive efficiency quantifies the capability of the propeller to convert the shaft power delivered by the engine into thrust. Again, adequate data is not available for counter-rotating propeller configurations as projected for the P-420. Instead, propeller efficiency is obtained through a multi-stage process according to published aircraft design practices. After Howe,<sup>5</sup> propulsive efficiency is calculated based on the advance ratio of the propeller. Corrections are employed as suggested by Raymer<sup>7</sup> for nacelle blockage, high blade-tip Mach numbers, and scrubbing drag due to the propeller slipstream.

Thrust is eventually determined as a function of engine power, propeller efficiency, and flight velocity (Eq. 4).

$$T = \frac{P_{eq} \eta_{effective}}{V} \quad (4)$$

#### D. Aircraft Performance

By combining the results of the above-described modules, the IDT conducts performance calculations covering considerations of the specific excess power (especially with regard to operating limitations), take-off and landing performance, and an analysis of the design-mission profile including diversion and loiter segments.

In a first step, based on a statistical estimation of mission-segment weight fractions,<sup>7</sup> an optimum flight condition for the initial cruise flight (at the top of climb (TOC)) is determined. With respect to minimum fuel consumption on a transport mission, the optimum condition is a maximum-range flight. For propeller configurations, this corresponds to a flight with minimum required thrust, i.e., maximum lift-to-drag ratio.<sup>7</sup> For the TOC of the P-420 at its designated cruise altitude of FL290, the optimum true airspeed is 195 m/s (379 kts), which corresponds to a Mach number of 0.64. In this condition, a maximum lift-to-drag ratio of 18.5 is attained.

In order to determine the operating envelope of the investigated aircraft, its specific excess power (SEP) is evaluated. In Fig. 6 the SEP contours of the P-420 with estimated initial cruise weight (TOC) are plotted over flight Mach number and altitude. All of the curves begin in the stall condition with the lowest possible Mach number for the respective altitude. From there, the SEP values increase with rising Mach numbers to distinctive maximums. The Mach numbers, at which these maximums are reached, rise with the flight altitude. Further increases in the Mach number lead to rapid decreases of the SEP values, as thrust diminishes and drag rises.

The outmost of the contours plotted in Fig. 6 reveals the aircraft's operating limitations as it represents the SEP approaching zero. The maximum operating Mach number of the P-420 is determined as 0.74. The maximum operating altitude is 32,200 ft while the service ceiling with a remaining climb capability of 100 ft/min is at 31,300 ft.

For the evaluation of take-off performance, a distinction is made between the normal case with all engines operating and the one-engine-inoperative case (OEI), which is especially relevant for certification regulations. Again, several different calculation methods are implemented in the IDT for the corresponding analysis. For a take-off with all engines operating, a simplified statistics-based approach is featured after Howe.<sup>5</sup> Torenbeek<sup>6</sup> provides a semi-empirical method, while detailed calculations are employed after Raymer,<sup>7</sup> who proposes a breakdown of take-off into different segment. For the baseline P-420 at maximum take-off weight, an all-engines-operating take-off distance of 2,157 m was determined with Raymer's method. The analysis of the OEI case yields the balanced field length (BFL), which is relevant for the assignment of the aircraft to the associated aerodrome reference codes

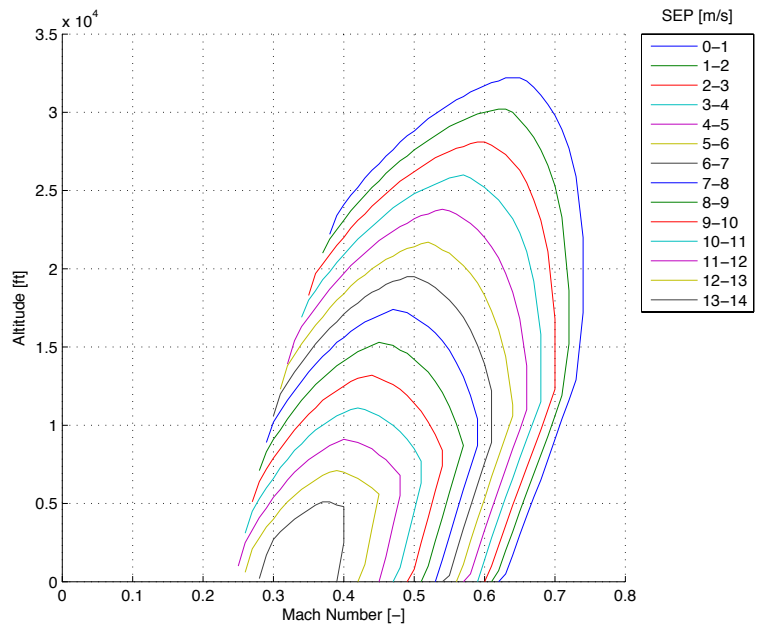


**Figure 6. SEP envelope contours of the baseline Propcraft P-420 concept with estimated initial cruise weight.** Colored lines represent different SEP value ranges.

(ARC). A method for calculation of the BFL is implemented in the IDT after Torenbeek and Raymer. A specialty in this context is that certification specifications require a minimum climb angle in the ‘second segment of take-off’ (i.e., the initial climb phase after the transition arc). For four-engine aircraft, a second-segment climb angle of  $1.7^\circ$  must be sustainable with one engine inoperative. The analysis of the P-420 revealed that this requirement could not be met by the baseline version of the concept and hence, a BFL could not be calculated.

The evaluation of the landing performance is similar to the one for the take-off case with methods after Howe, Torenbeek, and Raymer. A worst-case scenario of landing at maximum take-off weight is considered in order to assess whether a restriction should be imposed on the maximum permissible landing weight so as to comply with a particular ARC category. With the most detailed method (Raymer), a landing distance of 2,022 m is determined for the P-420. As this is inferior to the take-off distance, a restriction of the maximum landing weight is not necessary in this regard.

The main part of the aircraft performance module of the IDT features a detailed calculation of the projected design transport mission of the investigated aircraft. Each segment of the comprised standard-passenger-payload mission (SPP) and the subsequent diversion flight (see Fig. 7) is evaluated separately with regard to speed, duration, distance covered, and fuel burned. Where applicable, the IDT additionally calculates optimum flight conditions for specific segments, which yield minimum fuel burn. Comparison of the design mission specification to these optima allows for optimization of mission performance.

The corresponding evaluation of the P-420 revealed significant deficiencies in the projected design mission profile as it is depicted in Fig. 7. A considerable amount of fuel is consumed during taxiing, which is mainly due to the specification of extensive taxi times. Furthermore, climb performance is not satisfactory with a time to cruise altitude of 52 min, whereas the result for an optimized climb shows that a climbing time of only 30 min is attainable. Eventually, it was found that the design mission range of the baseline P-420 with standard payload was only 1,423 NM (2,635 km), which is 445 NM (825 km) less than the previously projected range of 1,868 NM (3,460 km) and actually fails the design requirement of 1,620 NM (3,000 km).

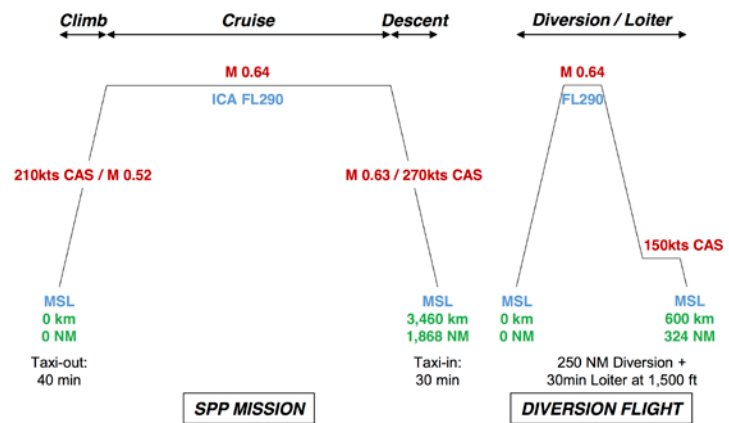


Figure 7. Design mission profile of the baseline Propcraft P-420 concept. Numerical values represent the characteristics projected during the conceptual phase.

### III. Requirements-Driven Design Iterations

#### A. Identification of Design Drivers

Based on an analysis of the Propcraft P-420 with the IDT as described above, it was discovered that the performance of the baseline concept was not satisfactory. Both, design requirements and certification specifications were not met to a sufficient degree.

In particular, the take-off performance in the second-segment climb was found critical. In this situation, thrust has diminished significantly due to the aircraft’s velocity (cf. Eq. 4). On the other hand, drag is high, as a relatively high lift coefficient is necessary and high-lift devices are deployed. The criticality is increased even further, as certification requires considering the OEI case. As previously stated, it was found that the baseline P-420 was not certifiable, because it failed the second-segment climb requirement. Hence, this is a major driver for the installed thrust-to-weight ratio, and adjustments need to be made here.

A second aspect regarding take-off performance is the field length. In the conceptual phase of the P-420, an ARC category 3 was projected, which restricts the field length to 1,800 m. The analysis of the all-engines take-off yielded a total take-off distance 20% greater. Moreover, the ARC requirement is actually based on the BFL, i.e., the one-engine-inoperative case, which could not be evaluated for the baseline P-420, but is obviously worse than with all engines operating. Similar to the take-off distance, also the predicted total landing distance exceeds the initial goal of 1,800 m. Hence, it has to be constituted that the projected ARC category 3 cannot be met unless greater changes to the concept are introduced. Instead, ARC category 4 applies. This is not a severe drawback, however, as most transport aircraft today fall under this category.

The analysis of the design mission revealed that the design mission range of 1,620 NM (3,000 km) is failed with the projected payload and mission fuel. Segmental assessment suggests, though, that this is caused to a certain extent by an unfavorable definition of the climb procedure and by the specification of extensive taxi times. With either modifications of these specifications or a slightly reduced passenger payload in favor of more mission fuel, the required range is achievable.

An overview of some critical design requirements of the Propcraft P-420 and the achieved performance of the baseline concept is provided in the constraint diagram in Fig. 8. It was created with the IDT and shows the design point of the baseline configuration with its wing loading and thrust-to-weight ratio together with colored lines representing different requirements and constraints.

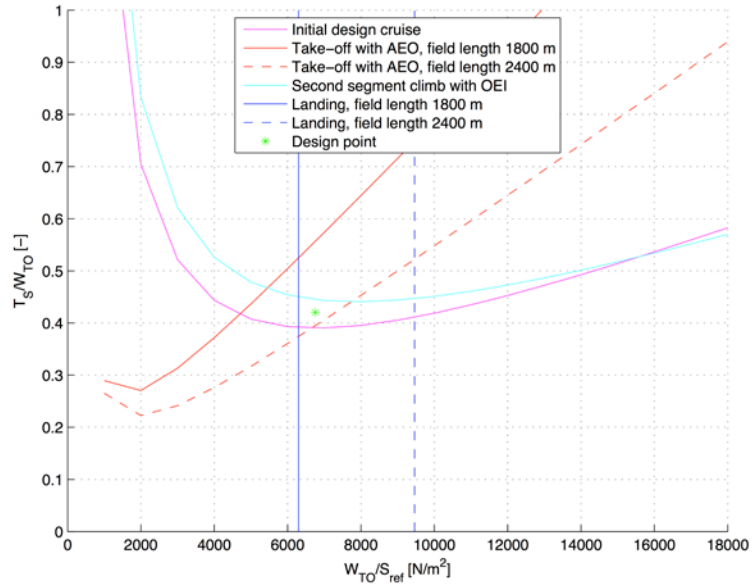


**Figure 8. Constraint diagram of the baseline Propcraft P-420 concept.** Colored lines represent different requirements and constraints.

## B. Design Iterations

In order to address the performance problems, design iterations were carried out with the IDT and the P-420 concept was developed further. A focus was on the propulsion characteristics, as the identified design drivers ‘take-off performance’ and ‘mission fuel consumption’ are both related to the propulsion system. Furthermore, the design mission specifications are reviewed and adapted to gain the optimum performance of the aircraft concept.

As the take-off analysis revealed, in the second-segment climb, the difference between thrust and drag of the baseline P-420 was not sufficient to maintain a minimum climb rate in the one-engine-inoperative case. A simple solution would be to increase the power rating of the engines, but this implies extended part-load operation in other flight conditions, which generally deteriorates efficiency. A more effective approach is to allow the engine power to be increased by ram effects not only at high flight altitudes, but also on the ground and during climb. As shown in Fig. 5, the engine model features a torque limit that restricted power to the value of the static MSL power rating. This torque limit represents a maximum acceptable stress level in the power train of the engine, i.e., spools, gearboxes, and propeller drive. The value of this limit can be considered as a technological parameter of the engine. The data of the Allison engine<sup>12</sup> show a torque limit at about 110% of its static MSL power rating. This characteristic is transferred to the power model of the revised Propcraft P-420 concept, which yields a torque limit of 10,670 kW. With this higher torque limit, the available power in the second-segment climb with one-engine inoperative at a Mach number of 0.27 is increased by about 5%.

A second aspect regarding the propulsion system concerned the propulsive efficiency of the propeller. With the employed calculation method, a value of 0.856 was obtained for the cruise flight condition. This is appraised fairly moderate, as consulted references state typical efficiencies of modern propellers ranging from 0.85 to 0.92.<sup>6,13</sup> Additionally, the P-420 is projected with dual counter-rotating propellers. However, the propeller efficiency calculation of the IDT is based on conventional propellers. For such counter-rotating configurations, efficiencies of 0.9 in cruise flight have been reported feasible.<sup>14,15</sup> In order to align the propeller efficiency estimation of the P-420 with these references, a fudge factor is introduced to the prediction method for the revised concept and tuned to yield a propeller efficiency of approximately 0.9 in the design cruise condition.

Besides engine power and propeller efficiency, the assumed specific fuel consumption was reviewed. It was found that the reference value of the equivalent power-specific fuel consumption that had been adopted during the initial development of the P-420 concept was actually quite ambitious, as consulted references state about 15% higher values.<sup>13,14</sup> The calibration of the employed fuel consumption model was thus updated correspondingly. A new reference value was specified based on data of the EPI TP400 turboprop available at the institute. As this engine of the Airbus A400M is rated at 8.2 MW of shaft power and features a modern design, it is considered a good reference for the current level of technology of powerful turboprop engines.



Moreover, the design mission specifications of the baseline Propcraft P-420 were revised based on the determined performance characteristics of the concept with regard to fuel-efficient flight operations. In particular, the revealed unfavorable specifications were corrected. Extensive taxi times were reduced to reasonable values of 15 minutes for both taxi-out and taxi-in, as suggested by Raymer.<sup>7</sup> Furthermore, the airspeed for the climb to cruise altitude had been set too low at a value of 210 kts (cf. Fig. 7), which resulted in a long climbing time with an increased fuel burn. Based on the calculation of an optimum climb, a constant speed of 231 kts was identified as an optimum value. For best overall climb performance, the constant Mach number for the second phase of the climb to cruise altitude was changed from 0.52 to 0.58. Besides, a revision of the fuel reserve requirements revealed that the projected diversion flight of 250 NM is actually only required for long range aircraft. As the Propcraft P-420 is a short- to medium-range concept, it only needs to provide reserves for a 200 NM diversion. Finally, the airspeed during loiter was adjusted. Again, the previously adopted 150 kts (cf. Fig. 7) had been set too low and resulted in an increased fuel burn. On the basis of an evaluation of optimum loitering with minimum required power, the optimum speed was identified as 196 kts and specified in the mission profile accordingly.

### C. Results

After undergoing the above-described design iterations, the revised Propcraft P-420 was eventually evaluated certifiable. It is now capable of fulfilling the climb requirement in the second segment of take-off with one engine inoperative, as a climb angle of  $2.2^\circ$  can be sustained in that case. The take-off field length with all engines operating was determined as 2,018 m, while the OEI case yielded a BFL of 3,452 m. For landing, the required field length of 2,022 m remains unchanged. Due to increased thrust, the evaluation of operating limitations resulted in a slightly extended operating envelope with a service ceiling of 32,300 ft and a maximum operating Mach number of 0.75.

Regarding mission performance, the increased engine power and higher propeller efficiency are compensated by the increased fuel consumption. A payload-range diagram of the revised P-420 is shown in Fig. 9. With a design payload of 420 passengers and five tons of cargo, a range of 1,592 NM (2,948 km) can be attained. To meet the design requirement of a minimum range of 1,620 NM (3,000 km), the payload has to be reduced to 416 passengers, which yields a mission range of 1,621 NM (3,003 km). As the original payload requirement specified a minimum passenger number of only 300, the reduction from 420 to 416 is considered acceptable, though. With a typical passenger load factor of 80%, the mission range can be extended to 2,347 NM (4,347 km).

In this case, the revised Propcraft P-420 achieves a specific fuel consumption of 3.07 l/PAX/100 km, which surpasses the average value of the German airliner fleet in 2013 by roughly 17%.<sup>16</sup> Hence, with the carried-out investigation using the IDT, it was found that the P-420 concept promises to ease congestion on highly frequented short- to medium-range air routes, while increasing fuel efficiency and thus mitigating the environmental impact compared to current aircraft types. The energy-consumption advantages of the concept are thereby merely attributed to the specific design as a high-capacity aircraft for short- to medium-range operations, as novel technologies were not considered in the concept and remain complementary.

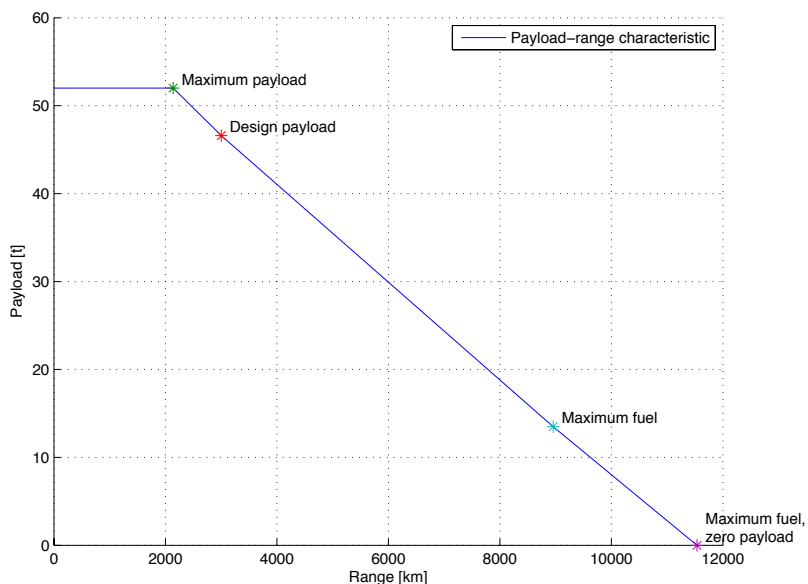


**Figure 9. Payload-range diagram of the revised Propcraft P-420 concept.** Based on the revised design mission profile and allowing for reserves of 10% of the enroute time, a 200 NM diversion and a 30 min loiter.

## IV. Conclusion

In addition to the design results addressing the Propcraft P-420, the analysis and redesign of the concept have led to the development of the IDT. With this tool, a consistent tool chain is now available at the institute for design studies and concept evaluations of large turboprop aircraft. Furthermore, the tool allows for quantification of sensitivities of an aircraft concept to parameter variation with respect to its design requirements and constraints.

Due to its modular structure, the IDT incorporates different aircraft design methods that range from initial statistics-based estimation to sophisticated high-fidelity analysis. Besides, this approach provides opportunities for further development of the tool and extension projects to enhance its functionalities.

## References

- <sup>1</sup>Airbus S.A.S., *Future Journeys: Global Market Forecast 2013-2032*, Blagnac Cedex, France, 2013.
- <sup>2</sup>Kenway, G. K. W., Henderson, R., Hicken, J.E., Kuntawala, N.B., Zingg, D. W., Martins, J. R. R. A. and McKeand, R.G., "Reducing Aviation's Environmental Impact Through Large Aircraft For Short Ranges," *48th AIAA Aerospace Sciences Meeting and Exhibit*, 2010.
- <sup>3</sup>Randt, N. P., "Foundations of a Technology Assessment Technique Using a Scenario-Based Fleet System Dynamics Model," *AIAA Aviation Technology, Integration, and Operations Conference*, 2013.
- <sup>4</sup>Iwanizki, M., Randt, N. P. and Sartorius, S., "Preliminary Design of a Heavy Short- and Medium-Haul Turboprop-Powered Passenger Aircraft," *52nd AIAA Aerospace Sciences Meeting and Exhibit*, 2014.
- <sup>5</sup>Howe, D., *Aircraft Conceptual Design Synthesis*, Professional Engineering Publishing, London and Bury St Edmunds, United Kingdom, 2000.
- <sup>6</sup>Torenbeek, E., *Synthesis of Subsonic Airplane Design*, Delft University Press, Martinus Nijhoff Publishers, Delft, The Hague, The Netherlands, 1982.
- <sup>7</sup>Raymer, D. P., *Aircraft Design: A Conceptual Approach*, 5th Edition, AIAA Education, Reston, VA, 2012.
- <sup>8</sup>Lowry, J. G. and Polhamus, E. C., *A Method for Predicting Lift Increments due to Flap Deflection at Low Angles of Attack in Incompressible Flow*, NACA Technical Note 3911, Langley Field VA, 1957.
- <sup>9</sup>Finck, R. D., Ellison, D. E. and Malthan, L. V., *USAF Stability and Control DATCOM*, Flight Dynamics Laboratory, Air Force Wright Aeronautical Laboratories, Air Force Systems Command, Wright-Patterson Air Force Base, OH, 1978.
- <sup>10</sup>Nita, M. and Scholz, D., 2012. "Estimating the Oswald Factor from Basic Aircraft Geometrical Parameters," *Deutscher Luft- und Raumfahrtkongress*, German Society for Aeronautics and Astronautics (DGLR), 2012.
- <sup>11</sup>Torenbeek, E., *Advanced Aircraft Design*, John Wiley & Sons Ltd, Chichester, West Sussex, United Kingdom, 2013.
- <sup>12</sup>Nicolai, L. M., Carichner, G. E., *Fundamentals of Aircraft and Airship Design*, Rev. and expanded ed., AIAA Education, Reston, VA, 2012.
- <sup>13</sup>Bräunling, W. J. G., *Flugzeugtriebwerke: Grundlagen, Aero-Thermodynamik, ideale und reale Kreisprozesse, Thermische Turbomaschinen, Komponenten, Emissionen und Systeme [in German]*, 3rd Edition, Springer-Verlag, Berlin, Heidelberg, Germany, 2009.
- <sup>14</sup>Zimmer, H., *Luftfahrttechnisches Handbuch: Triebwerkstechnologie [in German]*, Ausgabe A, Dornier Luftfahrt GmbH, Friedrichshafen, Germany, 1994.
- <sup>15</sup>Aerosila, *The SV-27 feathering-reversible puller coaxial hydromechanic propfan* [online], Stupino, Moscow, Russia, 2012, URL: [http://en.aerosila.ru/index.php?actions=main\\_content&id=32](http://en.aerosila.ru/index.php?actions=main_content&id=32) [accessed 26 August 2014].
- <sup>16</sup>BDL, *Energieeffizienz und Klimaschutz Report 2014 [in German]*, Bundesverband der Deutschen Luftverkehrswirtschaft BDL, Berlin, Germany, 2014.